

AA Long Term Note 14

TRADING MOMENTUM AGAINST BETATRON ACCEPTANCE
FOR AN UPGRADED ANTIPROTON COLLECTOR

C.D. Johnson

1. INTRODUCTION

In Long Term Note 7 E. Jones and R. Sherwood propose to improve the antiproton yield in the AA by increasing the efficiency of \bar{p} collection into the existing transverse acceptance. Gains of up to a factor 3 are theoretically attainable, although the practical difficulties are considerable. To go beyond this factor we have to contemplate enlarging, either directly or indirectly, the longitudinal and/or transverse machine acceptances. This note looks at the basic limitations of the gains to be had from these changes.

2. LONGITUDINAL AND TRANSVERSE MOMENTUM DEPENDENCE OF \bar{p} PRODUCTION DENSITY

J. Allaby¹⁾ has reviewed the experimental data on antiproton production from p-p and p-N collisions. His summaries of the relevant data from Amaldi et al.²⁾ and Eichten et al.³⁾ are reproduced in figures 1 and 2.

In fig. 1 the \bar{p} production density, $W(p,\theta)$ at 4 GeV/c from 24 GeV/c p-N collisions (Be, Cu and Pb) are plotted as a function of the total transverse energy E_T , which is related to transverse momentum, p_T , by :

$$E_T = (m_p^2 + p_T^2)^{1/2} \quad (1)$$

where m_p is the antiproton rest mass (0.938 GeV).

The relation :

$$W(p,\theta)/W(p,0) = 710 * e^{-7E_T} \quad (2)$$

provides a good fit to the data for production from lead, whereas the copper data is better represented by :

$$W(p,\theta)/W(p,0) = 278 * e^{-6E_T} \quad (3)$$

The ratios $W(p,\theta)/W(p,0)$ for lead and copper are plotted in figures 3 and 4 respectively as functions of the laboratory production angle, θ . Also shown are the differential yields $dN_{\bar{p}}/d\theta$. The vertical scales in this scale are arbitrary. The maxima occur between 120 and 140 mrad.

Returning to fig. 2, we have the production density at $\theta = 0^\circ$, $W(p,0)$, plotted versus antiproton longitudinal lab. momentum, P_{LAB} . The p-p data at low momenta are calculated by kinematic reflection from the measured values at 3.3 GeV/c and above. The p-N data above 3.5 GeV/c are from Eichten et al. Those at low momenta are from the preliminary results of an experiment by Amman et al.⁴⁾. The data are consistent with the assumption that the momentum dependence of \bar{p} production from p-N collisions has the same form as for the p-p process. The overall yields are lower due to \bar{p} reabsorption in the target nuclei.

3. TARGET YIELDS

3.1. Transverse momentum dependence

To illustrate a couple of points relating to the dependence of antiproton yield on transverse acceptance it is necessary to consider the effects of target geometry. As an example I take a copper target 110 mm long, the length of the present production target. The 26 GeV/c proton beam is assumed to have a Gaussian density distribution with $2\sigma = 1.2$ mm. The yield from this target has been computed using a combined Monte Carlo and numerical integration method. The absorption lengths for 26 GeV/c protons and 3.5 GeV/c antiprotons in copper are taken to be 139 mm⁵⁾ and 128 mm⁶⁾ respectively.

Fig. 5 shows the computed integrated antiproton yield versus θ^2 when the target has a diameter of 3 mm (curve 5). Also plotted are various limiting cases : curve 1 - constant $W(p,\theta)$ and no \bar{p} reabsorption, curve 2 - constant $W(p,\theta)$ and thick target (all \bar{p} 's exit through end of target), curve 3 - $W(p,\theta)$ as in fig. 4 but no \bar{p} reabsorption, and curve 4 - $W(p,\theta)$ as in fig. 4 but thick target. Note that the integrated yield from the 3 mm diameter target is quite close to the thick target approximation with constant $W(p,\theta)$ i.e. the yield is roughly proportional to θ^2 out to $\theta = 150$ mrad. This is due to the compensation of the fall-off in $W(p,\theta)$ by an increase in the number of \bar{p} 's escaping from the side of the target at larger production angles.

However, this does not mean that the antiproton yield will also be proportional to the square of the acceptance since these geometric factors also contribute to a dilution of transverse phase space density, which only non-linear or special focusing devices, as discussed in Note 7, can compensate.

In cylindrical coordinates the transverse phase plane referred to the downstream end of

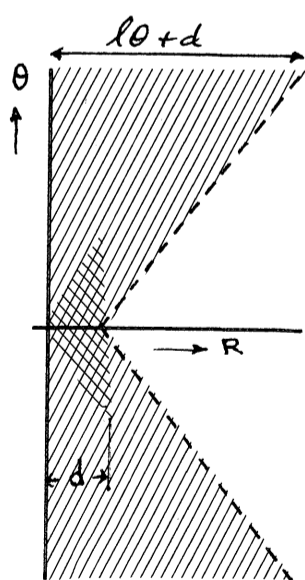


Fig. 6

$$p(\theta) \cong \frac{k\theta}{d} * \frac{d}{l\theta+d} = \frac{k\theta}{l\theta+d}$$

$p(\theta)$ = particle density
 l = target length
 d = beam size (uniform)
 k = constant

For $l\theta \gg d$

$$p(\theta) \rightarrow k/l = \text{const.}$$

the target is the familiar "butterfly" shown in fig. 6. In the central heavily shaded region the phase space density, determined largely by the proton beam size and distribution, is proportional to θ . At large θ the population of phase space is diluted by the effect of target length and the phase space density becomes approximately uniform. Thus, whereas initially the increase in yield with aperture at small apertures follows a quadratic dependence the trend is towards a linear relationship at larger apertures. This can be

offset a little by varying the matching parameters with aperture, but some device such as the focusing target is needed to maintain the quadratic dependence.

3.2. Longitudinal momentum dependence

In the lab. system the formula for the yield of antiprotons per interaction into the solid angle $\Delta\Omega$ and momentum bite Δp is :

$$N_{\bar{p}} = \Delta\Omega * \Delta p * p^2/2E * W(p,\theta) \quad (4)$$

In terms of momentum acceptance, $\Delta p/p$, this becomes :

$$N_{\bar{p}} = \Delta\Omega * \Delta p/p * p^3/2E * W(p,\theta) \quad (5)$$

Because of the kinematic term, $p^2/2E$, in equation 4 the yield per interaction from the AA target peaks at a little over 4 GeV/c, whereas the yield into fixed $\Delta p/p$ is at a maximum between 5 and 6 GeV/c. These relationships are plotted in fig. 7.

$W(p,0)$ is flat around 3.5 GeV/c. $W(p,0) * p^2/2E$ varies by about 10% over a 10% range in momentum around 3.5 GeV/c. For a fixed momentum acceptance the yield increases with antiproton momentum mainly because of the increased momentum bite. The behaviour of yield into fixed $\Delta p/p$ around the value $p = 3.5$ GeV/c is shown in fig. 8. A gain in yield of 5% per 0.1 GeV/c increase in \bar{p} momentum is predicted.

4. CONCLUSIONS

An upgraded antiproton collector can be expected to give an increase in yield proportional to its momentum acceptance and a little extra could be gained by operating at a higher \bar{p} momentum.

The benefits from increased transverse acceptance are more difficult to assess and are influenced more by target geometry than the fall-off in production density with angle. We should not expect much more than a linear gain in \bar{p} yield with aperture $(A_H * A_V)^{1/2}$.

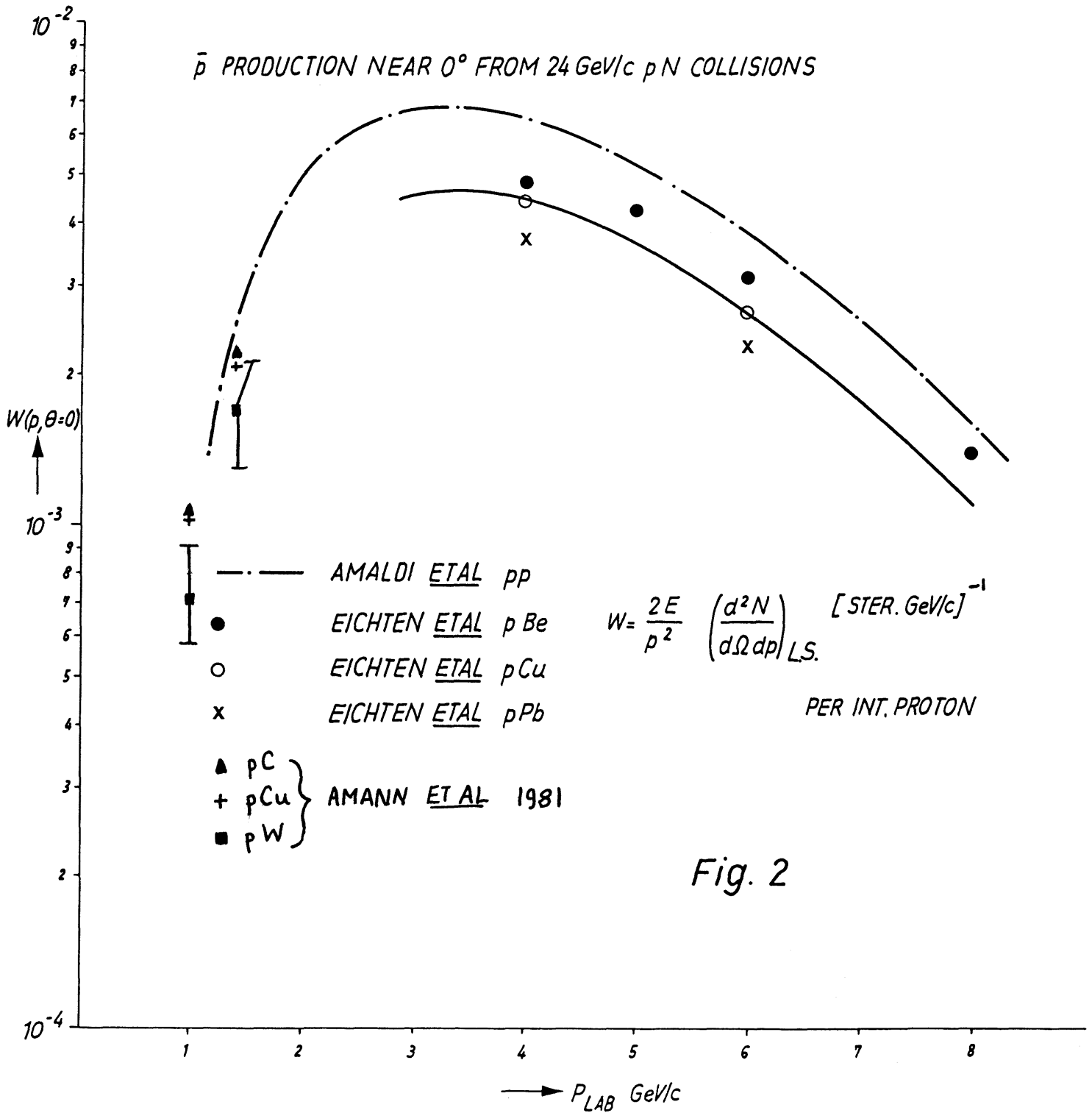
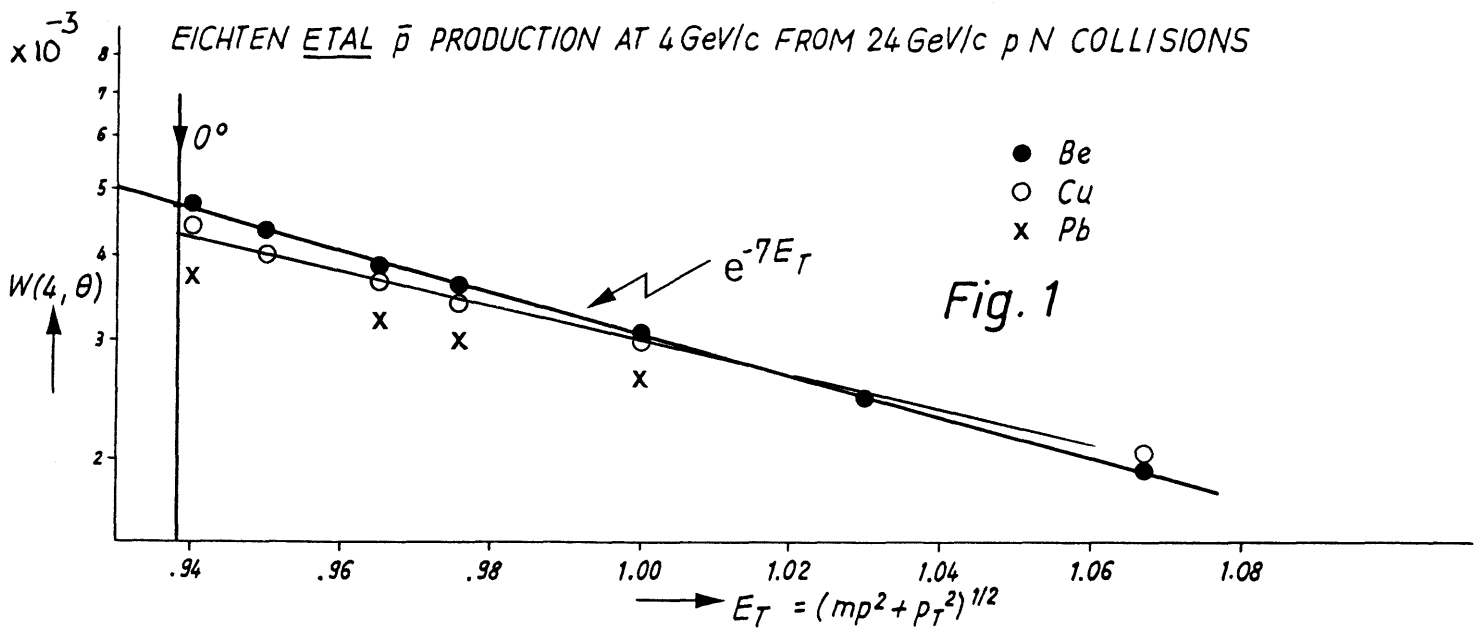
Something better than a linear lens system downstream from the target is required.

5. RADIATION ASPECTS OF IMPROVED PERFORMANCES

Any transport line from target to collector accepting a given $\Delta p/p$ will transmit with reduced acceptance particles outside the desired momentum bite. Increasing the transverse acceptance will make this situation worse and in general increase the radiation problem. Enlarging the momentum acceptance will for the most part mean taking in particles which would otherwise be lost outside the target area. As the majority of particles involved are π^- these will decay within the machine instead of being lost by interactions at the various aperture limits. This will tend to reduce the radiation shielding problem.

REFERENCES

- 1) \bar{p} Production at the AA, J.V. Allaby, Internal memorandum, (1981).
- 2) Momentum Spectra of Secondary Particles Produced in Proton-Proton Collisions at 14.2, 19.2 and 24.0 GeV/c, U. Amaldi et al., Nuclear Physics B86, 403-440, (1975).
- 3) Particle Production in Proton Interactions in Nuclei at 24 GeV/c, T. Eichten et al., Nuclear Physics B44, 333-343, (1972).
- 4) J. Amann et al., CERN-Los Alamos-TRIUMF Collaboration Experiment to Measure π^{\pm} , K^{\pm} , and p^{\pm} Production from C, Cu and W Targets by Protons of 10, 18 and 24 GeV/c, (1981). To be published.
- 5) Proton-Nuclei Cross-Sections at 20 GeV, G. Bellettini et al., Nuclear Physics 79, 609-624, (1966).
- 6) Absorption Cross-Sections for Pions, Kaons, Protons and Antiprotons on Complex Nuclei in the 6 to 60 GeV/c Momentum Range, S.P. Denisov et al., Nuclear Physics B61, 62-76, (1973).



EICHTEN ETAL \bar{p} PRODUCTION AT 4 GeV/c FROM 24 GeV/c pCu COLLISIONS

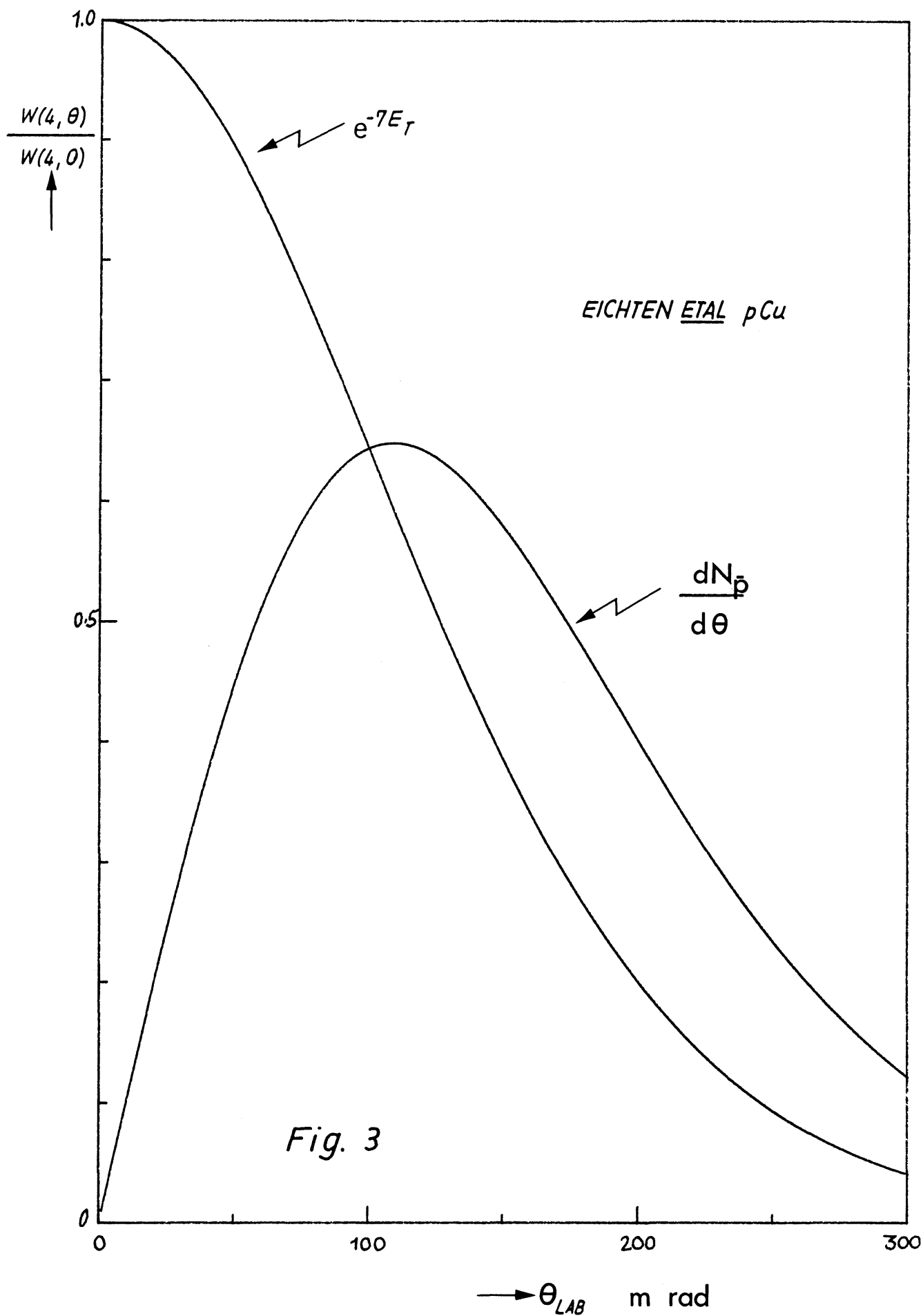
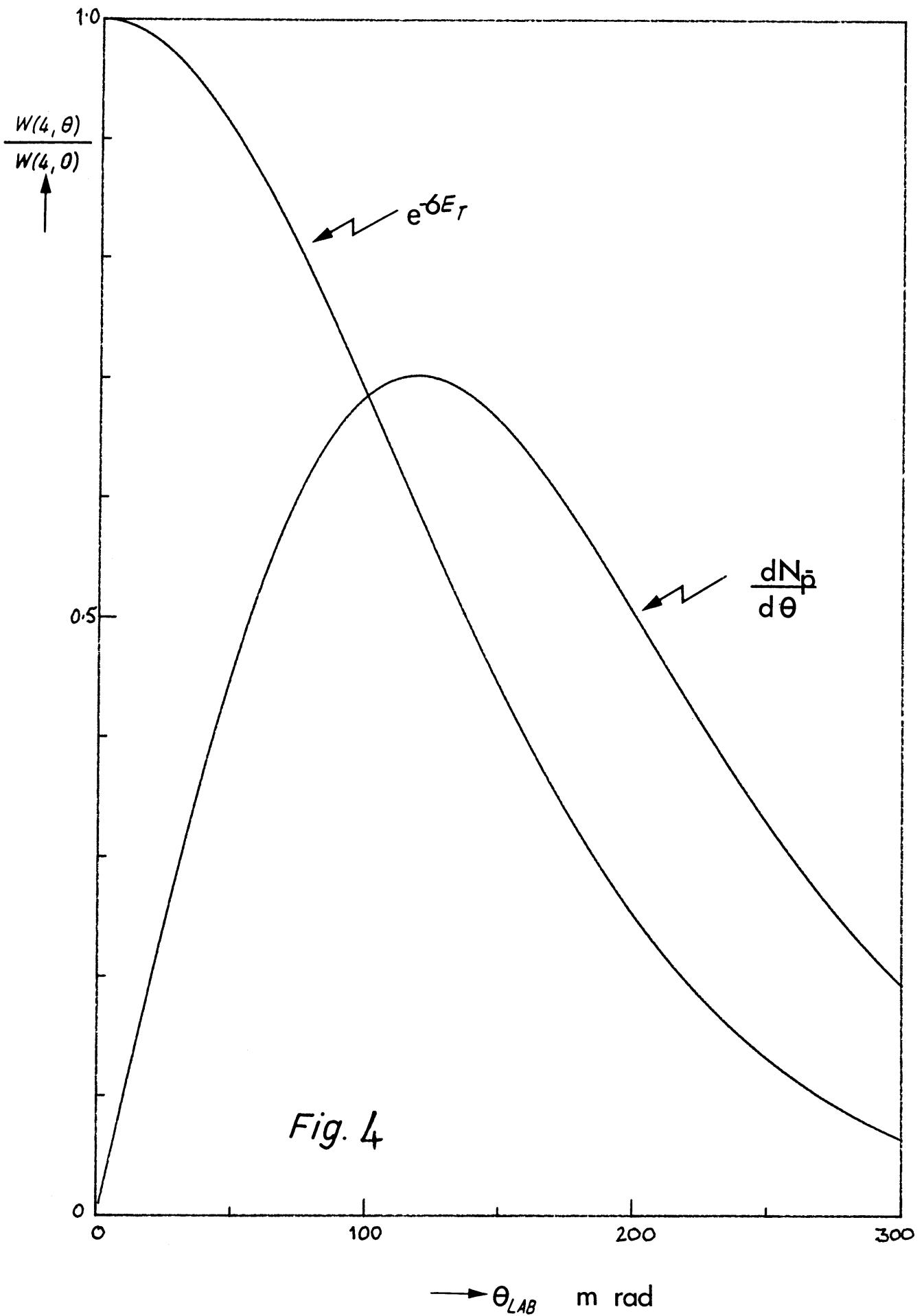
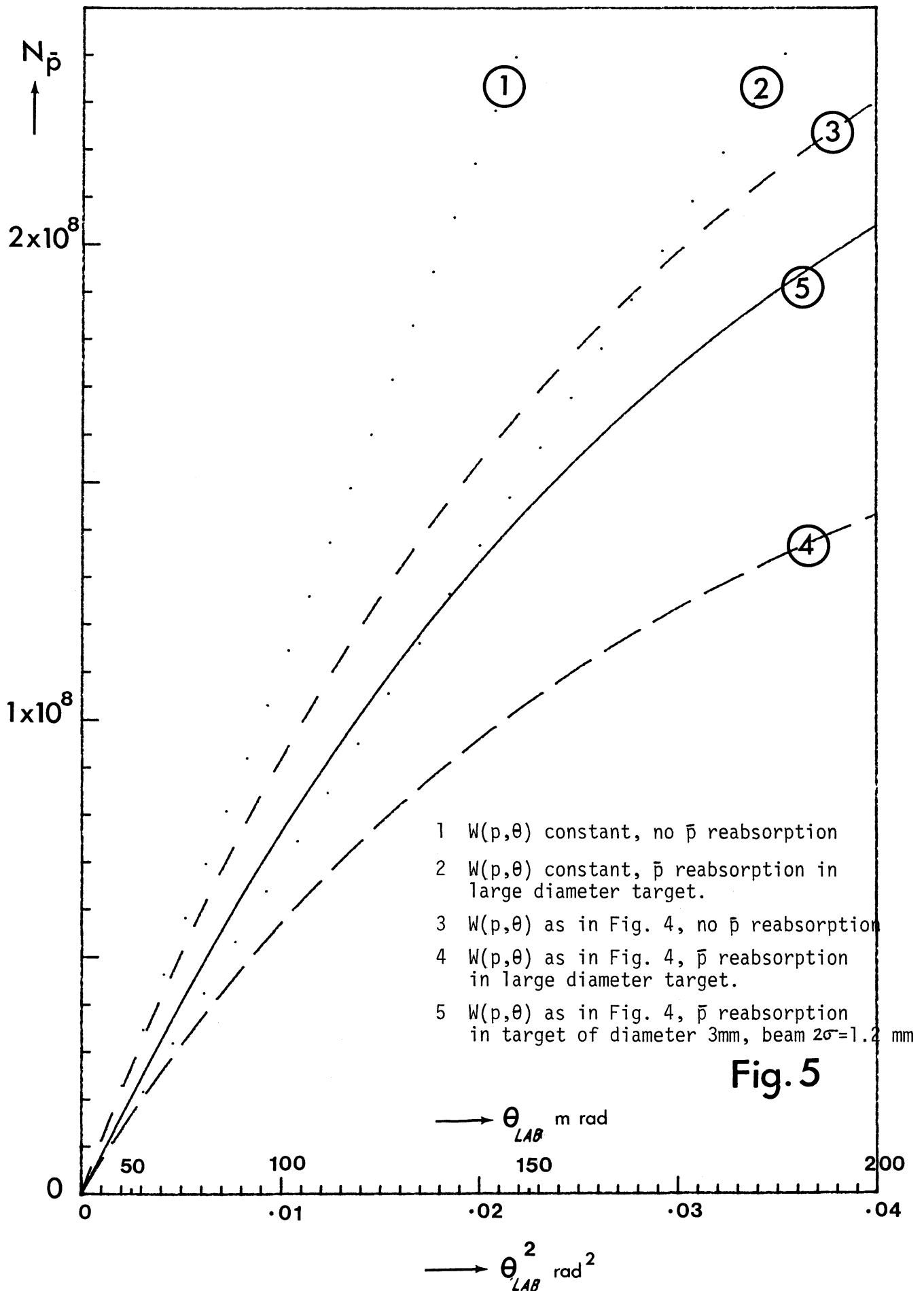


Fig. 3

EICHTEN ETAL \bar{p} PRODUCTION AT 4 GeV/c FROM 24 GeV/c pCu COLLISIONS



INTEGRATED ANTIPROTON YIELD VERSUS THE SQUARE OF THE LAB. PRODUCTION ANGLE, θ , FOR 10^{13} 26 Gev/c PROTONS ONTO A COPPER TARGET. Length=110mm



\bar{p} PRODUCTION NEAR 0° FROM 24 GeV/c pN COLLISIONS

$$W(p,0) * P^3 / 2E$$

$$W(p,0) * P^2 / 2E$$

$$\frac{\Delta P}{P} \approx 0.1$$

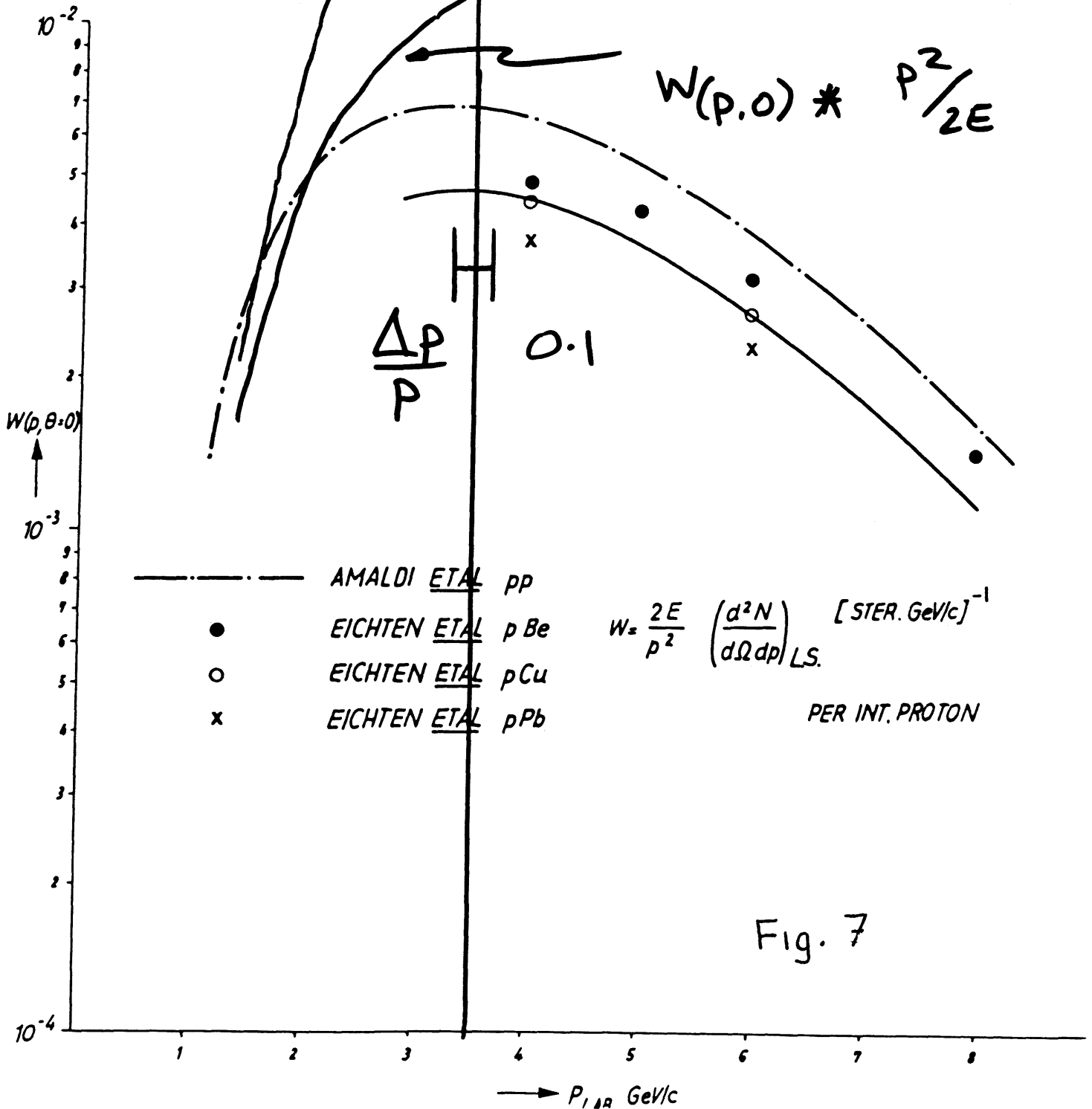


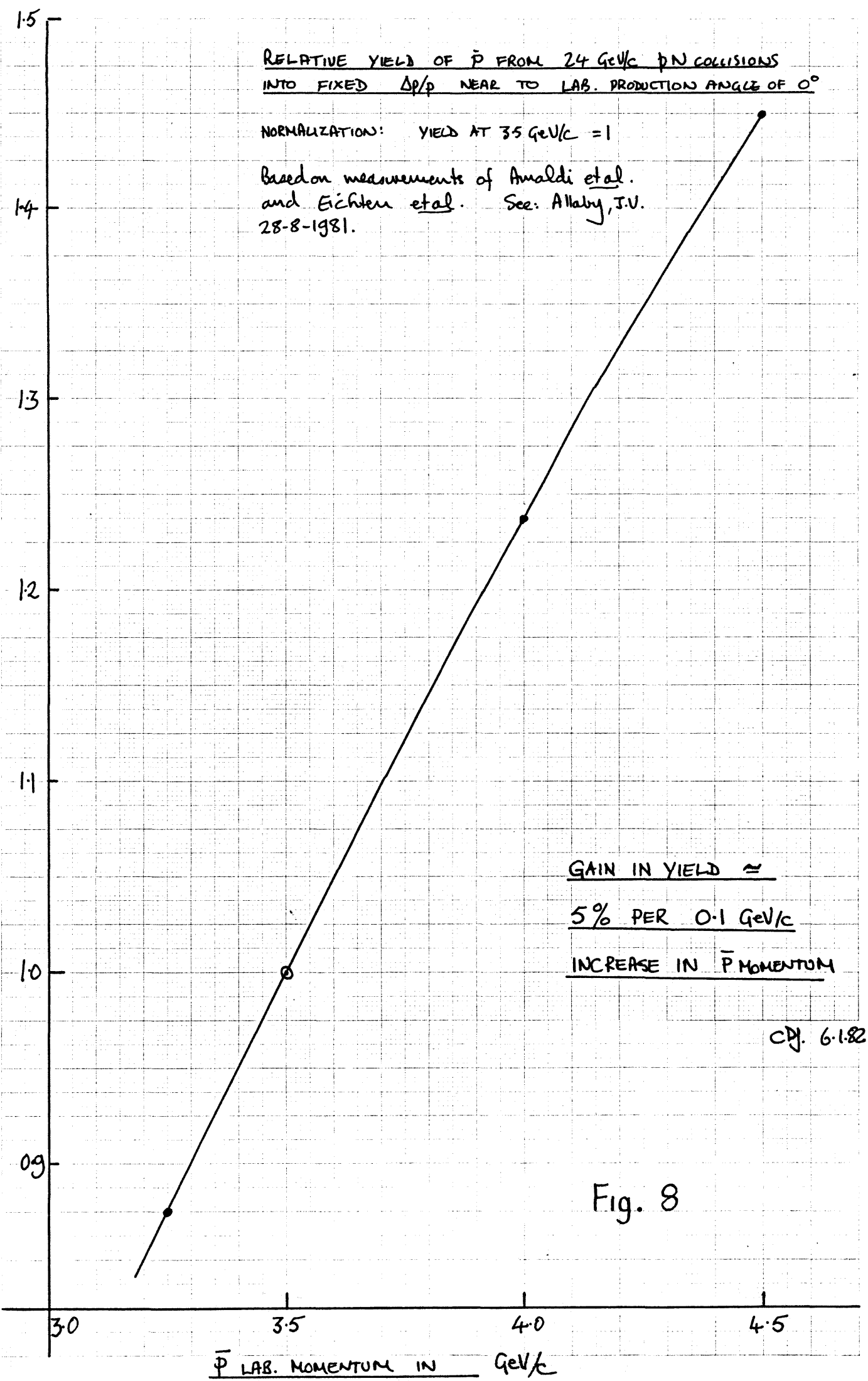
Fig. 7

RELATIVE YIELD OF \bar{p} FROM 24 GeV/c pN COLLISIONS
INTO FIXED $\Delta p/p$ NEAR TO LAB. PRODUCTION ANGLE OF 0°

NORMALIZATION: YIELD AT 3.5 GeV/c = 1

Based on measurements of Analdi *et al.*
and Eichten *et al.* See: Allaby, J.V.
28-8-1981.

RELATIVE YIELD INTO FIXED $\Delta p/p$
(YIELD AT 3.5 GeV/c = 1)



GAIN IN YIELD \approx
5% PER 0.1 GeV/c
INCREASE IN \bar{p} MOMENTUM

CDJ. 6.1.82

Fig. 8